A new uranyl phosphate sheet in the crystal structure of furongite

Fabrice Dal Bo[1,*], Frédéric Hatert[1] and Simon Philippo[2]

[1] Laboratoire de Minéralogie, B18, Université de Liège, 4000 Liège, Belgium
*Corresponding author, e-mail: fhatert@ulg.ac.be
[2] Section Minéralogie, Musée national d'histoire naturelle, Rue Münster 25, 2160 Luxembourg, Luxembourg

Abstract: The crystal structure of furongite, $Al_4[(UO_2)_4(PO_4)_6](OH)_2(H_2O)_{19.5}$, from the Kobokobo pegmatite, Kivu, Democratic Republic of Congo, was solved for the first time. Furongite is triclinic, the space group $P\bar{1}$, $Z = 2$, $a = 12.1685(8)$, $b = 14.1579(6)$, $c = 17.7884(6)$ Å, $\alpha = 79.822(3)$, $\beta = 77.637(4)$, $\gamma = 67.293(2)°$, and $V = 2746.2(2)$ Å^3. The crystal structure was refined from single-crystal X-ray diffraction data to $R_1 = 0.0733$ for 7716 unique observed reflections, and to $wR_2 = 0.2081$ for all 12,538 unique reflections. The structure of furongite contains infinite uranyl phosphate sheets of composition $[(UO_2)_4(PO_4)_6]^{10-}$ which are parallel to (1 0 1). The sheets are constituted by UrO$_5$ pentagonal bipyramids and PO$_4$ tetrahedra which share edges and vertices, and adjacent sheets are linked by a dense network of hydrogen bonds. Running through the sheets and connected mainly to the free apical oxygen atom of PO$_4$ tetrahedra are Al octahedra connected together to form remarkable $Al_2O_5(OH)(H_2O)_5$ and $Al_4O_8(OH)_2(H_2O)_{10}$ clusters. These Al clusters are only bonded to one sheet, and do not connect two adjacent sheets together. The topology of the uranyl phosphate sheets is related to the uranophane anion topology, and can be described as a new geometrical isomer of the uranophane group. Furongite is the first uranyl phosphate reported in nature with a U:P ratio of 2:3.

Key-words: furongite; crystal structure; Kobokobo; aluminium; uranyl phosphate; topology.

1. Introduction

At the end of the 1950's, the Kobokobo pegmatite, Kivu, Democratic Republic of Congo, was one of the largest beryllium deposits in the world. This pegmatite has produced a huge amount of beryl, columbite, cassiterite, and also contains important concentrations of phosphates with a unique uranium-thorium mineralization. A geological and mineralogical description of the different zones of the Kobokobo pegmatite has been provided by Safiannik-off & van Wambeke (1967). Uranium and thorium are found in the albite-beryl zone of the pegmatite, in which Th- and Pb-rich uraninite (4–5 wt% ThO$_2$) and U-rich zircon are occurring. During the last step of the pegmatite crystallization, phosphate-rich fluids have altered the primary feldspars as well as uraninite and zircon, allowing the formation of minerals of the phosphuranylite and autunite groups. The pegmatite of Kobokobo is the type locality for wakefieldite-(Ce), CeVO$_4$ (Deliens & Piret, 1986), kobokoboite, $Al_6(PO_4)_4(OH)_6(H_2O)_{11}$ (Mills *et al.*, 2010), and for twelve radioactive aluminium phosphates (Table 1). Among these occur two very rare species containing thorium as a major constituent: eylettersite, $Th_{0.75}Al_3(PO_4)_2(OH)_6$ (van Wambeke, 1972), and althupite, $AlTh(UO_2)_7(PO_4)_4O_2(OH)_5(H_2O)_{15}$ (Piret & Deliens, 1987). The crystal structures of actinides-bearing minerals discovered in the Kobokobo pegmatite are only known for five minerals: phuralumite (Piret *et al.*, 1979),

threadgoldite (Khosrawan-Sazedj, 1982), upalite (Piret & Declercq, 1983), vanmeersscheite (Piret & Deliens, 1982), and althupite (Piret & Deliens, 1987).

Furongite was originally described from the oxidation zone of the Furong uranium deposit, Hunan province, China (Hunan Team, 1976), with the proposed chemical formula $Al_{13}(UO_2)_7(PO_4)_{13}(OH)_{14}(H_2O)_{58}$. The crystal structure was not investigated and the unit-cell parameters were refined from X-ray powder diffraction data in the space group $P1$: $a = 19.227$, $b = 14.094$, $c = 12.102$ Å, $\alpha = 67.21$, $\beta = 115.64$, and $\gamma = 94.51°$ (Hunan Team, 1976, 1979). Deliens & Piret (1977) have reported a mineral similar to furongite, named "minéral F", from the pegmatite of Kobokobo. Optical properties and crystallographic data indicate that "minéral F" from Kobokobo and furongite from Furong belong to the same mineral species (Deliens & Piret, 1985a). However, some discrepancy remains about the chemical formula of furongite; Deliens & Piret (1985a) have reported the formula $Al_2(UO_2)_2(PO_4)_3(OH)(H_2O)_{13.5}$ for the specimen from Kobokobo, while the simplified formula of the Chinese furongite is approximately $Al_2(UO_2)(PO_4)_2(OH)_2(H_2O)_8$. The huge difference in the oxide weights, especially for UO$_3$, is not explained in this paper. Shen & Peng (1981) announce to have solved the structure of furongite in a communication to the 12nd Congress of the International Union of Crystallography (1981), but this communication remains unavailable and no scientific paper about their structural results has been published. Consequently, as the

Table 1. List of actinide-bearing minerals discovered in the Kokobobo pegmatite, Kivu, DRC.

Mineral	Formula	S.G.	a (Å)/α (°)	b (Å)/β (°)	c (Å)/γ (°)	Ref.
Uranium-bearing minerals						
Kamitugaite*	$PbAl(UO_2)_5(PO_4)_2(OH)_9(H_2O)_{9.5}$	$P1/P\bar{1}$	10.98/95.1	15.96/96.1	9.07/89.0	1
Metavanmeersscheite*	$U^{6+}(UO_2)_3(PO_4)_2(OH)_6(H_2O)_2$	$Fddd$	34.18/90	33.88/90	14.07/90	2
Moreauite*	$Al_3(UO_2)(PO_4)_3(OH)_2(H_2O)_{13}$	$P2_1/c$	23.41/90	21.44/92.0	18.34/90	3
Mundite*	$Al(UO_2)_3(PO_4)_2(OH)_3(H_2O)_{5.5}$	$P2_1cn/Pmcn$	17.08/90	30.98/90	13.76/90	4
Phuralumite	$Al_2(UO_2)_3(PO_4)_2(OH)_6(H_2O)_{10}$	$P2_1/a$	13.87/90	20.92/112.4	9.43/90	5
Ranunculite*	$Al(UO_2)(PO_3OH)(OH)_3(H_2O)_4$	M	11.10/90	17.7/90	18.0/90	6
Threadgoldite	$Al(UO_2)_2(PO_4)(OH)(H_2O)_8$	$C2/c$	20.17/90	9.84/110.7	19.72/90	7
Triangulite*	$Al_3(UO_2)_4(PO_4)_4(OH)_5(H_2O)_5$	$P1/P\bar{1}$	10.39/116.4	10.56/107.8	10.60/113.4	8
Upalite	$Al[(UO_2)_3(PO_4)_2O(OH)](H_2O)_7$	$P2_1/a$	13.70/90	16.82/111.5	9.33/90	5
Vanmeersscheite	$U^{6+}(UO_2)_3(PO_4)_2(OH)_6(H_2O)_4$	$P2_1mn$	17.06/90	16.76/90	7.02/90	2
Thorium-bearing minerals						
Althupite	$AlTh(UO_2)_7(PO_4)_4O_2(OH)_5(H_2O)_{15}$	$P\bar{1}$	10.95/72.6	18.57/68.2	13.50/84.2	9
Eylettersite*	$Th_{0.75}Al_3(PO_4)_2(OH)_6$	$R\bar{3}m$	6.98/90	6.98/90	16.66/120	10

* Unknown crystal structure. *M*: monoclinic. References: 1. Deliens & Piret (1984). 2. Piret & Deliens (1982); 3. Deliens & Piret (1985b); 4. Deliens & Piret (1981); 5. Deliens & Piret (1979a); 6. Deliens & Piret (1979b); 7. Deliens & Piret (1979c); 8. Deliens & Piret (1982); 9. Piret & Deliens (1987); 10. van Wambeke (1972).
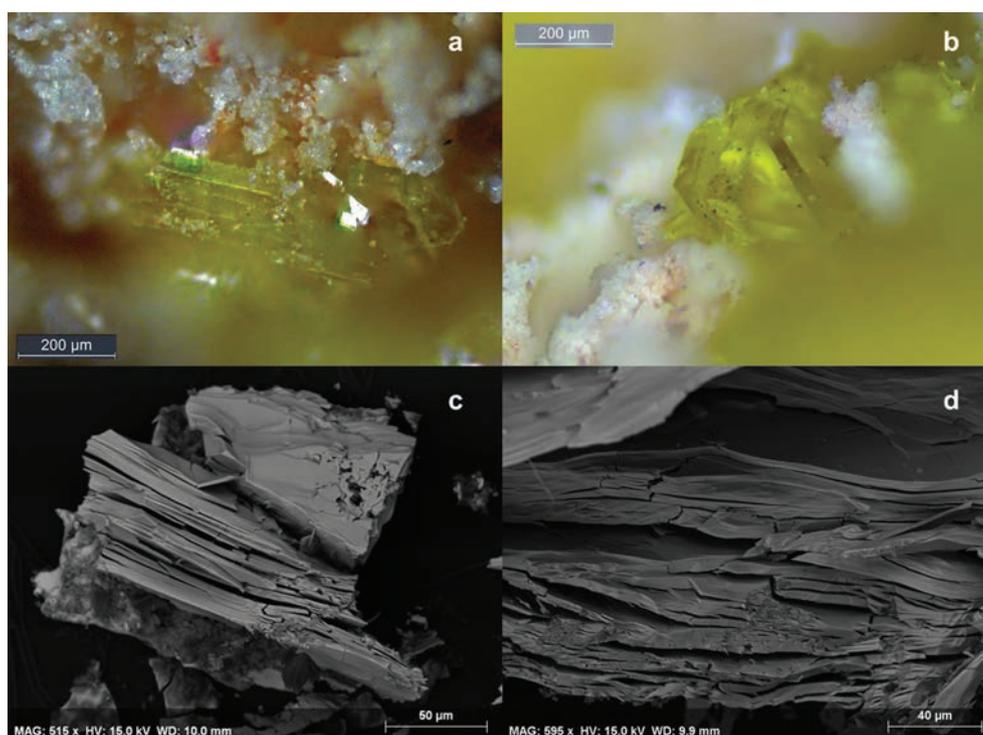
Fig. 1. Images of the analysed specimens. (a) and (b): deep yellow flattened crystals of furongite. (c) and (d): backscattered-electron images of furongite showing the stacking of very thin plates. Photographs (a) and (b) by R. Warin.

mineralogical data about furongite remain scarce, we have decided to reinvestigate samples from Kobokobo in order to determine the crystal structure of furongite and to confirm its chemical formula.

2. Sample description

Furongite occurs as deep yellow, transparent to translucent crystals, ranging up to 0.3 mm in maximum dimension (Fig. 1). The crystals form multiple intergrowths; they are flattened and terminated by faces forming an arrow head.

Some intergrowths are constituted by very thin plates (Fig. 1c and d). The sample used (VC2053) in the current study was collected in the Kokobobo pegmatite and belongs to the collection of the "Musée National d'Histoire Naturelle du Luxembourg."

3. Chemical composition

Energy-dispersive X-ray spectroscopy (EDS) was used to confirm the chemical composition of furongite. The crystals were mounted on adhesive carbon tape, carbon-
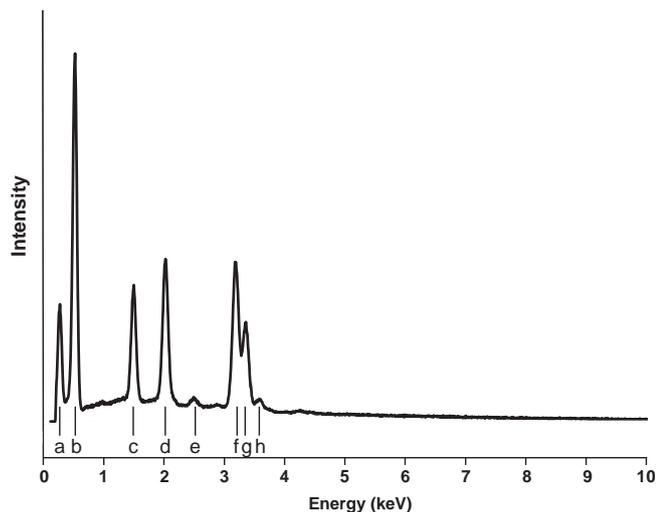
Fig. 2. Energy-dispersive X-ray emission spectra of furongite. The labelled EDS peaks correspond to the following lines: a, $CK\alpha$; b, $OK\alpha$; c, $AlK\alpha$; d, $PK\alpha$; e, $UM\zeta$; f, $UM\alpha$; g, $UM\beta$; h, $UM\gamma$.

Table 2. Experimental details for the single-crystal X-ray diffraction study of furongite, Kobokobo, DRC.

Structural formula	$Al_4[(UO_2)_4(PO_4)_6](OH)_2$ $(H_2O)_{19.5}$
a (Å)	12.1685(8)
b	14.1579(6)
c	17.7884(6)
α (°)	79.822(3)
β	77.637(4)
γ	67.293(2)
V (Å^3)	2746.2(2)
Space group	$P\overline{1}$
Z	2
D_{calc} (g cm^{-3})	2.515
Absorption coefficient (mm^{-1})	12.100
$F(000)$	2016
Radiation (Å)	$MoK\alpha$, 0.71073
Crystal size (mm)	$0.12 \times 0.10 \times 0.07$
Colour	deep golden yellow
Temperature (K)	293(2)
θ range (°)	2.04–28.21
Reflection range	$-16 \leq h \leq 13$
	$-17 \leq k \leq 17$
	$-23 \leq l \leq 23$
Total no. of reflections	24,379
Unique reflections	12,538
Observed reflections, $|F_o| \geq 4\sigma_F$	7716
Refined parameters	586
R_1, $|F_o| \geq 4\sigma_F$	0.0733
R_1, all data	0.1288
wR_2 (F^2), all data	0.2081
GOF obs/all	1.051/1.051
$\Delta\sigma_{min}$, $\Delta\sigma_{max}$ (e/Å^3)	3.62, -3.20

coated and analysed by an environmental scanning electron microscope (FEX XL30 ESEM-FEG) working in high vacuum mode, using 15 kV accelerating potential. The only chemical elements detected are U, P, Al, and O (Fig. 2). No other elements, especially elements prone to substitute P (As), Al (Fe), and OH group (F), were detected.

4. X-ray crystallography and structure determination

4.1. Single-crystal X-ray diffraction and structure solution

The single-crystal X-ray study of furongite was carried out with a Rigaku Oxford Diffraction Xcalibur four-circle diffractometer (kappa geometry), using $MoK\alpha$ radiation ($\lambda = 0.71073$ Å, 40 kV, 40 mA), and equipped with an EOS CCD area detector, on a $0.12 \times 0.10 \times 0.07$ mm crystal fragment (sample VC2053). Furongite is triclinic, $P\overline{1}$, with $a = 12.1685(8)$, $b = 14.1579(6)$, $c = 17.7884(6)$ Å, $\alpha = 79.822(3)$, $\beta = 77.637(4)$, $\gamma = 67.293(5)°$, $V = 2746.4(2)$ Å^3, and $Z = 2$ (Table 2). The data were corrected for Lorentz, polarization and absorption effects, the latter with an empirical method using the SCALE3 ABSPACK scaling algorithm included in the CrysAlis RED software package (Agilent Technologies, 2012). The crystal structure of furongite was solved by direct methods and subsequently refined using SHELX and SHELXL software (Sheldrick, 2008, 2015). The reflection conditions and statistics clearly indicate the space group $P\overline{1}$, consistent with the data previously reported by Deliens & Piret (1985a). Scattering curves for neutral atoms and anomalous dispersion correction were taken from the *International Tables for X-ray Crystallography, Vol. C* (Wilson, 1992).

The structure of furongite was solved by direct methods and refined successfully on the basis of F^2 for all unique data in space group $P\overline{1}$. Structure model including anisotropic displacement parameters for all non-H atoms converged and gave an agreement index ($R1$) of 7.73%, calculated for the 7716 observed unique reflections ($|F_o| \geq 4\sigma_F$). The relative occupancy of the Al and P sites were freely refined in order to detect the result of some cationic substitutions. As the relative occupancy of all Al and P sites remained very close to unity, these sites were assigned complete occupancy by Al and P, respectively. This observation is consistent with the presence of only Al, P and U in furongite, as observed by EDS analyses. The occupancy factor of the O47 to O61 sites was set to 0.5, in order to keep their isotropic atom displacement parameters in acceptable value. The refinement of the structure converged with final indices of agreement $wR_2 = 0.2081$ for all data using structure-factor weights assigned during least-squares refinement. Final atom coordinates, isotropic atom displacement parameters and site occupancies are given in Table 3, and selected interatomic distances are reported in Table 4. Bond-valence sums (BVS) were calculated using the parameters of Brown & Altermatt (1985) for Al and P, and those of Burns *et al.* (1997) for U^{6+}. The BVS values vary between 2.76 and 2.90 valence units (*vu*) for the Al sites, between 4.88 and 5.10 *vu* for the P sites, and between 6.06 and 6.50 for the U site. Further details of the crystal structure investigation are available from the

Table 3. Atom fractional coordinates, isotropic displacement parameters ($Å^2$), site occupancies and bond-valence sums (*vu*) for furongite.

	x	y	z	U_{iso}	Occ.	BVS
Al1	0.5757(5)	0.6212(4)	1.0324(3)	0.0209(12)	1	2.90
Al2	0.8714(5)	0.5476(4)	1.0318(3)	0.0230(12)	1	2.76
Al3	1.1959(5)	0.1366(4)	0.7164(3)	0.0223(12)	1	2.87
Al4	0.9729(6)	0.0554(5)	0.7058(3)	0.0363(15)	1	2.86
U1	0.56405(7)	0.63531(5)	1.35751(4)	0.02207(18)	1	6.24
U2	1.44584(7)	−0.12498(5)	0.61294(4)	0.02193(18)	1	6.26
U3	0.64665(7)	0.36495(5)	1.27539(4)	0.02209(18)	1	6.50
U4	0.87076(6)	0.13488(5)	1.03195(4)	0.02107(18)	1	6.07
P1	1.2213(5)	−0.0912(3)	0.7557(3)	0.0241(11)	1	5.07
P2	1.4079(5)	0.1405(3)	0.5828(3)	0.0247(11)	1	4.95
P3	1.5176(5)	−0.3969(3)	0.5633(3)	0.0264(12)	1	4.89
P4	0.7457(4)	0.3901(3)	1.0731(2)	0.0195(10)	1	5.02
P5	0.6665(5)	0.6175(3)	1.1802(2)	0.0199(10)	1	5.10
P6	0.9888(5)	0.1199(3)	0.8586(3)	0.0227(11)	1	5.00
O1	0.9839(13)	0.1695(9)	1.0578(7)	0.031(3)	1	1.64
O2	1.1086(12)	0.1262(9)	0.8156(6)	0.028(3)	1	1.81
O3	0.6375(12)	0.5354(8)	1.2419(17)	0.026(3)	1	2.18
O4	0.9054(13)	0.2162(9)	0.9002(7)	0.033(3)	1	1.65
O5 (H_2O)	1.1263(13)	0.2873(9)	0.7202(8)	0.037(4)	1	0.38
O6 (H_2O)	0.9017(11)	0.6768(9)	1.0172(7)	0.029(3)	1	0.39
O7	1.4792(13)	−0.3754(9)	0.4842(7)	0.034(4)	1	1.93
O8	0.6267(11)	0.4814(8)	1.0687(6)	0.023(3)	1	1.77
O9	0.4226(13)	0.6880(9)	1.3285(7)	0.031(3)	1	1.81
O10	0.7915(12)	0.5746(9)	1.1361(7)	0.029(3)	1	1.82
O11	0.7763(13)	0.3336(9)	1.3150(6)	0.030(3)	1	1.84
O12	1.2793(11)	−0.0091(8)	0.7164(6)	0.019(3)	1	1.88
O13	0.7567(12)	0.3471(8)	1.1573(6)	0.026(3)	1	1.97
O14	1.3304(13)	−0.0728(9)	0.5569(7)	0.037(4)	1	1.79
O15	1.0991(12)	0.0612(10)	0.7363(7)	0.032(3)	1	1.97
O16	1.2246(12)	−0.1117(9)	0.8420(7)	0.030(3)	1	1.89
O17	1.6526(14)	−0.4423(11)	0.5590(8)	0.044(4)	1	1.35
O18 (OH)	1.0709(10)	0.1357(8)	0.6743(6)	0.017(3)	1	1.04
O19 (OH)	0.7293(11)	0.6161(8)	0.9917(6)	0.022(3)	1	1.10
O20 (H_2O)	1.0069(17)	0.0180(13)	0.6019(9)	0.062(5)	1	0.44
O21	1.4625(12)	0.2047(8)	0.6134(6)	0.028(3)	1	1.85
O22 (H_2O)	0.5547(12)	0.5958(9)	0.9343(7)	0.028(3)	1	0.43
O23 (H_2O)	0.8718(16)	−0.0210(17)	0.7275(10)	0.078(6)	1	0.50
O24	0.7413(10)	0.3029(8)	1.0325(6)	0.016(2)	1	1.79
O25 (H_2O)	0.5102(12)	0.7684(9)	0.9945(7)	0.033(3)	1	0.39
O26	1.2740(12)	0.1648(9)	0.6188(7)	0.032(3)	1	1.76
O27	0.5179(12)	0.3961(8)	1.2367(7)	0.026(3)	1	1.91
O28 (H_2O)	1.0228(11)	0.4811(8)	1.0661(6)	0.023(3)	1	0.43
O29 (H_2O)	0.8331(16)	0.1687(15)	0.6726(10)	0.073(6)	1	0.41
O30	1.5571(12)	−0.1764(8)	0.6709(8)	0.034(3)	1	1.85
O31 (H_2O)	1.3237(11)	0.1299(9)	0.7676(7)	0.023(3)	1	0.43
O32	1.3135(11)	−0.1858(8)	0.7151(6)	0.023(3)	1	2.19
O33	0.6489(12)	0.7011(8)	1.2316(6)	0.025(3)	1	1.67
O34 (H_2O)	0.4118(12)	0.6289(10)	1.0669(7)	0.033(3)	1	0.44
O35	0.5732(11)	0.6601(8)	1.1258(7)	0.025(3)	1	1.85
O36	1.4564(12)	−0.2970(8)	0.6072(6)	0.027(3)	1	2.06
O37	1.4556(12)	−0.4670(8)	0.6203(6)	0.030(3)	1	2.10
O38	0.8532(11)	0.4209(8)	1.0361(6)	0.020(3)	1	1.81
O39	1.0150(11)	0.0349(8)	0.9285(6)	0.023(3)	1	1.72
O40	0.7086(15)	0.5841(10)	1.3796(7)	0.040(4)	1	1.87
O41	0.7622(11)	0.0992(8)	1.0062(6)	0.023(3)	1	1.78
O42	0.9225(14)	0.0978(12(	0.8055(8)	0.047(4)	1	1.86
O43	1.4808(11)	0.0262(8)	0.6031(7)	0.025(3)	1	1.97
O44	1.4124(13)	0.1641(9)	0.4947(7)	0.035(4)	1	1.88
O45 (H_2O)	0.9522(14)	0.3887(11)	0.8368(8)	0.047(4)	1	0
O46 (H_2O)	1.2313(14)	0.1320(11)	0.9389(8)	0.044(4)	1	0
O47 (H_2O)	0.738(3)	0.555(2)	0.8146(16)	0.041(7)	0.5	0
O48 (H_2O)	0.468(2)	0.8217(18)	0.8467(14)	0.029(6)	0.5	0
O49 (H_2O)	0.232(4)	0.543(3)	1.319(2)	0.092(13)	0.5	0

Table 3. (continued).

	x	y	z	U_{iso}	Occ.	BVS
O50 (H_2O)	0.148(3)	0.1172(19)	0.4986(15)	0.034(6)	0.5	0
O51 (H_2O)	0.746(3)	0.181(2)	0.5541(19)	0.060(9)	0.5	0
O52 (H_2O)	1.813(3)	−0.349(2)	0.5184(18)	0.055(9)	0.5	0
O53 (H_2O)	0.773(4)	−0.046(3)	0.887(2)	0.076(11)	0.5	0
O54 (H_2O)	0.980(4)	−0.254(3)	0.808(2)	0.088(13)	0.5	0
O55 (H_2O)	0.712(4)	0.008(2)	0.631(2)	0.094(14)	0.5	0
O56 (H_2O)	0.750(3)	−0.233(3)	0.857(2)	0.069(10)	0.5	0
O57 (H_2O)	0.793(3)	0.380(3)	0.492(2)	0.071(11)	0.5	0
O58 (H_2O)	0.523(3)	0.9190(19)	1.0611(15)	0.036(7)	0.5	0
O59 (H_2O)	1.063(3)	−0.176(2)	0.5849(16)	0.044(7)	0.5	0
O60 (H_2O)	0.286(3)	0.685(2)	1.2072(19)	0.059(9)	0.5	0
O61 (H_2O)	1.541(3)	−0.013(2)	0.7839(16)	0.042(7)	0.5	0
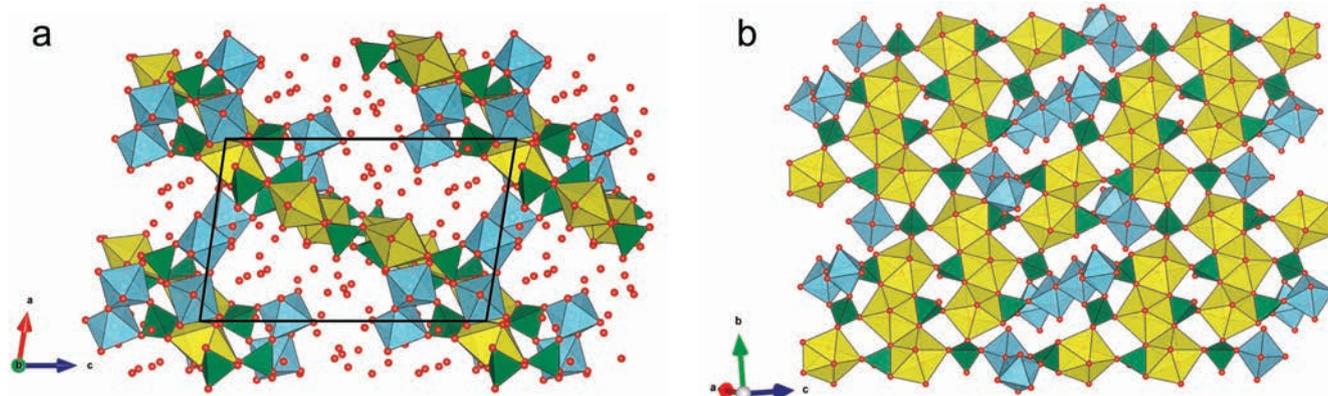
Fig. 3. General view of the structure of furongite (a) and of one isolated uranyl phosphate sheet (yellow and green, respectively) running parallel to (1 0 1) (b). The Al octahedra are blue, oxygen atoms, hydroxyl groups and water molecules are red. Unit-cell edges are outlined by the solid black line (VESTA 3 software; Momma & Izumi, 2011).

Fachinformationszentrum Karlsruhe, 76344 Eggenstein-Leopoldshafen, Germany, on quoting the depository number CSD-431291, the names of the authors and the citation of the paper.

4.2. Description of the crystal structure

The crystal structure of furongite contains four symmetrically independent U^{6+} cations which are forming typical nearly linear UO_2^{2+} uranyl ions (*Ur*). Each uranyl ion is coordinated by five additional oxygen atoms located in the equatorial planes of the uranyl ions to form UrO_5 pentagonal bipyramids. The $\langle U–O_{Ur}\rangle$ and $\langle U–O_{eq}\rangle$ (*eq* = equatorial) mean bond lengths vary between 1.72 and 1.77 Å, and between 2.35 and 2.40 Å, respectively (Table 4). These values closely match the typical bond lengths observed for [7] coordinated U^{6+} (Burns *et al.*, 1997). In addition to the UrO_5 polyhedra, six symmetrically independent P^{5+} cations are occurring as PO_4 tetrahedra. The $\langle P–O\rangle$ mean bond lengths vary between 1.53 and 1.54 Å. The UrO_5 pentagonal bipyramids and PO_4 tetrahedra share edges and vertices, yielding a $[(UO_2)_4(PO_4)_6]^{10−}$ sheet nearly parallel to (1 0 1) (Fig. 3). The uranyl phosphates sheets are crossed by four

symmetrically independent Al^{3+} cations occurring as octahedra: $Al1O_2OH(H_2O)_3$, $Al2O_2OH(H_2O)_3$, $Al3O_3OH(H_2O)_2$, and $Al4O_2OH(H_2O)_3$. These Al octahedra form by edge- and corner-sharing two kind of clusters − $Al_2O_5(OH)(H_2O)_5$ and $Al_4O_8(OH)_2(H_2O)_{10}$ (Fig. 4a and b), which are connected to the free apical oxygen atoms of the PO_4 tetrahedra, and to one equatorial oxygen atom of the $U2O_7$ pentagonal bipyramids (Fig. 4c). The hydroxyl groups (OH18 and OH19) are only shared between two Al octahedra (Fig. 4). In addition, the interlayer of the structure contains also seventeen isolated water molecules, fifteen of which have been treated as having an occupancy factor set to 0.5. The structural formula of furongite obtained from the refinement is $Al_4[(UO_2)_4(PO_4)_6](OH)_2(H_2O)_{19.5}$, which can be simplified as $Al_2[(UO_2)_2(PO_4)_3](OH)(H_2O)_{10}$.

5. Discussion

5.1. Comparison with previous works

The powder pattern of furongite calculated from the structural data collected on single crystal is given in Table 5 (PowderCell software; Kraus & Nolze, 1996). This powder pattern is very similar to the powder pattern reported by

Table 4. Selected bond distances (Å) for furongite.

U1–O9	1.743(14)	U2–O30	1.732(14)				
U1–O40	1.727(16)	U2–O14	1.747(16)	P1–O12	1.573(11)	P2–O21	1.536(12)
U1–O21	2.299(10)	U2–O12	2.662(10)	P1–O15	1.480(14)	P2–O43	1.536(12)
U1–O33	2.443(11)	U2–O32	2.429(11)	P1–O32	1.552(11)	P2–O44	1.538(14)
U1–O3	2.509(11)	U2–O36	2.409(10)	P1–O16	1.518(13)	P2–O26	1.543(14)
U1–O37	2.442(11)	U2–O43	2.310(11)	$\langle$P1–O$\rangle$	1.53	$\langle$P2–O$\rangle$	1.54
U1–O7	2.274(12)	U2–O44	2.274(12)				
$\langle$U1–O$_{Ur}\rangle$	1.73	$\langle$U2–O$_{Ur}\rangle$	1.74	P3–O36	1.577(11)	P4–O24	1.559(11)
$\langle$U1–O$_{eq}\rangle$	2.39	$\langle$U2–O$_{eq}\rangle$	2.40	P3–O37	1.574(12)	P4–O13	1.527(12)
				P3–O17	1.505(16)	P4–O8	1.531(12)
U3–O27	1.716(14)	U4–O1	1.794(14)	P3–O7	1.521(14)	P4–O38	1.517(12)
U3–O11	1.734(14)	U4–O41	1.751(12)	$\langle$P3–O$\rangle$	1.54	$\langle$P4–O$\rangle$	1.53
U3–O13	2.234(11)	U4–O24	2.292(10)				
U3–O32	2.373(10)	U4–O39	2.334(10)	P5–O33	1.545(11)	P6–O2	1.521(13)
U3–O36	2.441(11)	U4–O39^{i}	2.468(11)	P5–O10	1.497(13)	P6–O39	1.563(11)
U3–O3	2.346(11)	U4–O16	2.324(12)	P5–O3	1.543(12)	P6–O42	1.506(14)
U3–O37	2.376(10)	U4–O4	2.449(11)	P5–O35	1.524(13)	P6–O4	1.550(12)
$\langle$U3–O$_{Ur}\rangle$	1.72	$\langle$U4–O$_{Ur}\rangle$	1.77	$\langle$P5–O$\rangle$	1.53	$\langle$P6–O$\rangle$	1.53
$\langle$U3–O$_{eq}\rangle$	2.35	$\langle$U4–O$_{eq}\rangle$	2.37				
Al1–OH19	1.83(1)	Al2–OH19	1.85(1)	Al3–H$_2$O31	1.93(1)	Al4–OH18	1.89(1)
Al1–O8	1.87(1)	Al2–O10	1.93(1)	Al3–OH18	1.84(1)	Al4–O15	1.86(1)
Al1–H$_2$O34	1.92(1)	Al2–O38	1.88(1)	Al3–O12	1.91(1)	Al4–O42	1.87(1)
Al1–H$_2$O22	1.93(1)	Al2–H$_2$O28	1.93(1)	Al3–O2	1.87(1)	Al4–H$_2$O20	1.93(1)
Al1–H$_2$O25	1.97(1)	Al2–H$_2$O28^{i}	1.90(1)	Al3–H$_2$O5	1.98(1)	Al4–H$_2$O29	1.95(2)
Al1–O35	1.83(1)	Al2–H$_2$O6	1.96(1)	Al3–O26	1.85(1)	Al4–H$_2$O23	1.87(2)
$\langle$Al1–$\varphi\rangle$	1.89	$\langle$Al2–$\varphi\rangle$	1.91	$\langle$Al3–$\varphi\rangle$	1.90	$\langle$Al4–$\varphi\rangle$	1.89
O5–O2	2.64(2)	O28–O28	2.45(1)	O23–O42	2.67(3)	O45–O47	2.81(4)
O5–O18	2.77(2)	O28–O38	2.70(2)	O23–O53	2.85(4)	O46–O2	2.93(2)
O5–O19	2.95(4)	O19–O8	2.70(2)	O23–O55	2.73(5)	O46–O58	2.79(4)
O5–O26	2.61(2)	O19–O10	2.69(2)	O25–O19	2.70(2)	O47–O49	2.85(5)
O5–O31	2.74(2)	O19–O22	2.73(2)	O25–O34	2.69(2)	O48–O16	2.76(3)
O5–O45	2.77(2)	O19–O25	2.67(2)	O25–O35	2.64(2)	O48–O61	2.79(4)
O6–O1	2.99(2)	O19–O28	2.83(2)	O25–O48	2.71(3)	O49–O17	2.72(4)
O6–O10	2.75(2)	O19–O35	2.70(1)	O25–O58	2.68(3)	O49–O60	2.73(5)
O6–O19	2.70(2)	O19–O38	2.66(2)	O29–O9	2.99(3)	O50–O14	2.94(3)
O6–O28	2.65(2)	O20–O15	2.73(2)	O29–O42	2.68(2)	O50–O55	2.97(5)
O6–O28	2.67(2)	O20–O18	2.69(2)	O29–O51	2.67(4)	O51–O55	2.78(2)
O6–O38	2.79(2)	O20–O23	2.59(2)	O29–O60	2.98(4)	O51–O59	2.88(5)
O6–O46	2.72(2)	O20–O29	2.63(2)	O31–O12	2.58(2)	O52–O17	2.67(4)
O18–O2	2.62(2)	O20–O50	2.81(4)	O31–O26	2.76(2)	O52–O44	2.99(3)
O18–O12	2.73(2)	O20–O59	2.62(3)	O31–O33	2.54(2)	O53–O56	2.92(6)
O18–O15	2.73(2)	O22–O8	2.83(2)	O31–O61	2.68(4)	O54–O56	2.66(6)
O18–O20	2.69(2)	O22–O34	2.61(2)	O34–O8	2.64(2)	O55–O43	2.87(5)
O18–O26	2.62(2)	O22–O47	2.69(3)	O34–O24	2.64(2)	O57–O17	2.75(4)
O18–O29	2.75(3)	O23–O15	2.63(3)	O34–O35	2.62(2)	O58–O58	2.84(4)
O18–O42	2.74(2)	O23–O20	2.59(3)	O34–O60	2.71(3)	O59–O11	2.95(3)
O28–O10	2.73(2)	O23–O29	2.59(3)	O45–O4	2.72(2)		

Symmetry code: i −x, −y, −z.

Deliens & Piret (1985a) from Debye–Scherrer data, indicating that both samples are equivalent. Moreover, Deliens & Piret (1985a) have previously proved that the furongite from the Kobokobo pegmatite and the Furong deposit is the same mineral species. Table 6 compares the unit-cell parameters for furongite reported by Hunan Team (1976), Deliens & Piret (1985a) and in the present study. The unit-cell parameters measured by single-crystal X-ray diffraction closely match those calculated from powder diffraction by Hunan Team (1976). Transformation matrices are [0 0 $\overline{1}$, 0, $\overline{1}$ 0, $\overline{1}$ 0 0] (to Hunan Team, 1976) and [$\overline{1}$ 0 1, 0 1 0, 1 0 0] (to Deliens & Piret, 1985a).

5.2. Water content of furongite

The bond valence analysis of furongite indicates that two anionic sites of the structure are occupied by hydroxyl groups and twenty-seven anionic sites are occupied by water molecules (Table 3). Fifteen of the sites occupied by water molecules have an occupancy factor set to 0.5, giving a content of 19.5 water molecules. Such water content is not consistent with that inferred from thermogravimetric analyses by Deliens & Piret (1985a) (27 water molecules). However, an occupancy factor of 1 for all the O sites, occupied by water molecules, would
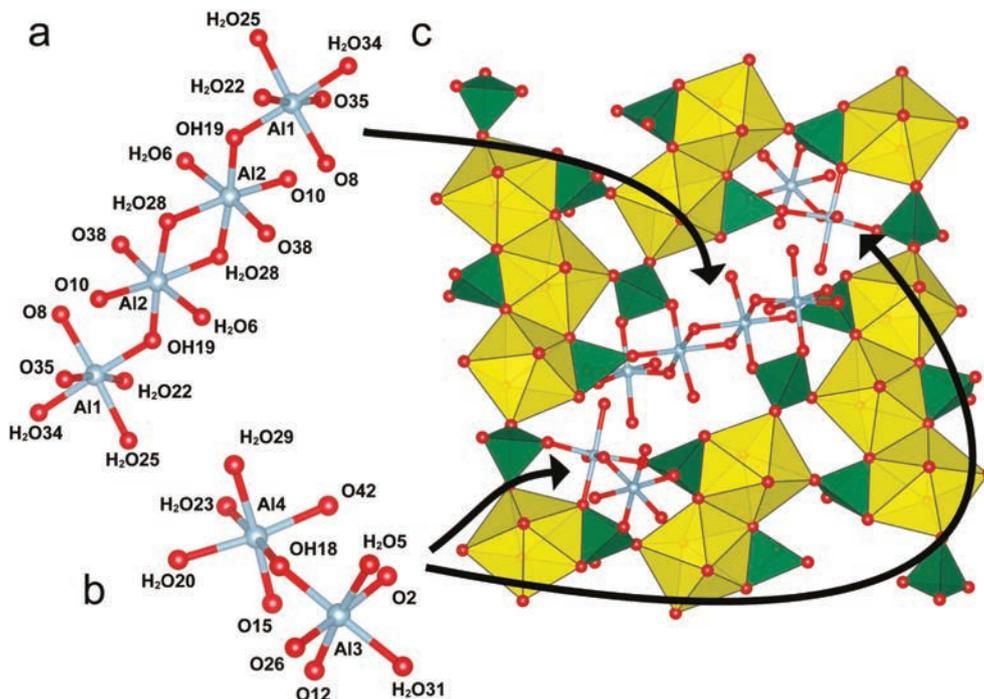
Fig. 4. Detailed view of the $Al_4O_8(OH)_2(H_2O)_{10}$ (a) and $Al_2O_5(OH)(H_2O)_5$ clusters (b), and of the connectivity between these clusters and the uranyl phosphate sheet (c).

lead to a total of 27 water molecules. This difference may be due to the loss of some weakly-bonded water molecules under the X-ray beam.

The H_2O groups have an essential role in the stability of the furongite structure, by connecting adjacent sheets together through H-bonds (Al clusters are not shared from one sheet to another). The detailed analysis of the hypothetical connectivity around the H_2O groups (Table 4) shows several tendencies. First, the H_2O groups connected to Al extend mainly H-bonds towards the O^{2-} atoms shared between UO_7 and PO_4 polyhedra. These O^{2-} atoms are slightly undersaturated in charge; therefore, it is very likely that they act as H-bonds acceptors. Also, H_2O groups bonded to Al seem to identically extend H-bonds towards other H_2O groups connected to Al, and towards isolated H_2O groups. Second, the OH^- groups extend H-bonds towards O^{2-} atoms from the sheets and H_2O groups connected to Al. Their specific positions inside the Al clusters prevent them to extend H-bonds towards isolated water molecules. Finally, the isolated H_2O groups, which are located in the interlayer space, identically extend H-bonds towards O^{2-} atoms from the sheets, towards both H_2O groups connected to Al, and towards other isolated H_2O groups. To sum up, the connectivity between adjacent sheets is mainly provided by the isolated H_2O groups, while the H_2O groups bonded to Al are mainly reinforcing the connectivity of the Al clusters to the uranyl phosphate sheets.

5.3. Structure relationships

The chemical composition and the structure of furongite are remarkable in several ways. In total, ten uranyl phosphates (or arsenates) with a U/P ratio <1 are reported in nature

(ulrichite, coconinoite, moreauite, hallimondite, parsonsite, walpurgite, phosphowalpurgite, orthowalpurgite, and lakebogaite); however, furongite is the only mineral showing a U:P ratio of 2:3. All the other mineral species have a U:P ratio of 1:2, excepted moreauite which has a U:P ratio of 1:3.

The chemical composition of the uranyl phosphate sheets occurring in furongite, $[(UO_2)_4(PO_4)_6]^{10-}$, has not been reported for any other uranyl mineral. These sheets can be built using two structural blocks: dimers and trimers of UO_7 pentagonal bipyramids, which are both linked by edge- and corner-sharing to PO_4 tetrahedra (Fig. 5). Dimers of edge-sharing pentagonal bipyramids are known in the structures of johannite Cu $(UO_2)_2(SO_4)_2(OH)_2(H_2O)_8$ (Mereiter, 1982), deliensite $Fe(UO_2)_2(SO_4)_2(OH)_2(H_2O)_7$ (Plášil *et al.*, 2012), plášilite $Na(UO_2)(SO_4)(OH)(H_2O)_2$ (Kampf *et al.*, 2015), vandenbrandeite $CuUO_2(OH)_4$ (Rosenzweig & Ryan, 1977), uranosphaerite $Bi(UO_2)O_2(OH)$ (Hughes *et al.*, 2003), and in minerals with a structure possessing the francevillite sheet-anion topology (Mereiter, 1986) (Fig. 6). Dimers of uranyl pentagonal bipyramids also occur in several synthetic uranyl compounds (Åberg, 1969; Serezhkina *et al.*, 1990; Almond *et al.*, 2002; Almond & Albrecht-Schmitt, 2004; Burns, 2005). In addition, the structures of hallimondite, $Pb_2[(UO_2)(AsO_4)_2](H_2O)_n$, parsonsite, $Pb_2[(UO_2)(PO_4)_2](H_2O)_n$ $(0 \leq n \leq 0.5)$ (Locock *et al.*, 2005), and lakebogaite $NaCaFe_2H(UO_2)_2(PO_4)_4(OH)_2(H_2O)_8$ (Mills *et al.*, 2008) are also built around dimers of pentagonal bipyramids and, in these structures, the connectivity between the dimers and the tetrahedra is exactly the same as in the structure of furongite (Fig. 6). In contrast, trimers of UO_7 pentagonal bipyramids are extremely

Table 5. X-ray powder diffraction data for furongite from Kobokobo (DRC).

			This study		Deliens & Piret (1985a)							This study		Deliens & Piret (1985a)		
h	k	l	d_{calc}	I	d_{calc}	d_{obs}	I	h	k	l	d_{calc}	I	d_{calc}	d_{obs}	I
1	0	0	11.08	18	11.07	11.15	40	0	$\bar{3}$	2	3.718	2	3.703	3.709	10
1	1	0	10.52	27	–	–	–	$\bar{1}$	$\bar{1}$	4	3.699	2			
1	1	1	10.11	4	10.12	10.08	100	3	2	3	3.620	5	3.635	3.638	50
1	0	1	10.09	100	10.09			1	4	1	3.518	7	–	–	–
$\bar{1}$	0	1	8.71	1	8.66	–	–	$\bar{2}$	2	1	3.508	2	3.504	3.504	40
$\bar{1}$	$\bar{1}$	1	8.16	2	8.15	8.04	15	2	4	1	3.462	4	3.461	3.461	30
1	1	2	7.62	1	7.57	7.52	10	2	4	2	3.402	2	3.387	3.387	10
1	$\bar{1}$	0	7.23	1	–	–	–	0	$\bar{1}$	5	3.256	2	3.267	3.264	50
1	2	1	6.80	2	6.80	6.79	25	0	4	0	3.247	7	3.260		
1	2	0	6.78	2	6.77			$\bar{2}$	0	4	3.169	2	3.173	3.175	15
$\bar{1}$	0	2	6.33	1	6.31	6.30	5	$\bar{1}$	0	5	3.158	1	–	–	–
2	1	1	6.03	5	6.02 / 6.01	6.02	30	3	4	2	3.106	3	3.078	3.086	15
0	0	3	5.76	10	5.77	5.73	30	$\bar{2}$	2	4	3.007	3	–	–	–
1	1	3	5.64	1	–	–	–	$\bar{3}$	$\bar{1}$	3	2.985	2	2.956 / 2.955	2.960	5
2	0	1	5.54	10	5.54 / 5.53	5.54	30	$\bar{3}$	0	3	2.904	1	–	–	–
2	1	2	5.48	3	–	–	–	$\bar{1}$	2	5	2.849	3	2.852	2.850	20
2	0	2	5.05	5	5.06	5.07	35	$\bar{1}$	2	5	2.831	4	2.811	2.813	40
1	2	3	4.92	3	4.92	4.92	15	1	$\bar{4}$	1	2.789	2	–	–	–
$\bar{1}$	$\bar{2}$	2	4.86	3	–	–	–	0	2	6	2.741	3	2.742	2.743	20
$\bar{2}$	$\bar{2}$	1	4.73	4	4.72 / 4.70	4.70	25	$\bar{2}$	2	4	2.711	2	–	–	–
$\bar{1}$	$\bar{1}$	3	4.61	1	–	–	–	1	3	6	2.671	1	2.673	2.675	20
0	2	3	4.55	3	4.55 / 4.54	4.54	15	$\bar{3}$	2	4	2.599	1	2.608	2.605	15
$\bar{1}$	$\bar{3}$	1	4.29	2	4.28	4.28	50	1	0	7	–	–	2.495	2.496	5
$\bar{1}$	2	2	4.26	5	4.27			$\bar{4}$	$\bar{2}$	3	2.427	1	2.425	2.424	10
0	$\bar{2}$	3	4.10	2	–	–	–	$\bar{2}$	0	7	2.131	1	2.128	2.129	10
0	3	2	4.04	1	–	–	–	0	6	3	2.100	1	2.105	2.104	10
3	2	0	3.86	2	3.85	3.85	5	$\bar{1}$	0	8	2.059	1	2.060	2.060	5
$\bar{1}$	$\bar{3}$	2	3.81	1	–	–	–	$\bar{1}$	6	2	1.971	1	1.973	1.973	15
								1	6	6	1.930	0.5	1.932	1.933	5
								$\bar{4}$	$\bar{6}$	3	1.857	0.6	1.863	1.862	3
								0	6	6	1.824	0.6	1.815	1.814	20

Table 6. Comparison of the crystallographic parameters for furongite

Locality	Furong	Kobokobo	Kobokobo
S.G.	$P1$	$P1$ or $P\bar{1}$	$P\bar{1}$
a (Å)	17.87	19.271(6)	12.168(1)
b	14.18	14.173(4)	14.158(1)
c	12.18	12.136(7)	17.789(1)
α (°)	67.8	67.62(3)	79.82(1)
β	77.5	115.45(3)	77.64(1)
γ	79.9	94.58(3)	67.29(1)
V (Å^3)	2710	2752(2)	2746.4(2)
Z	1	4	2
d_{calc}	2.92	2.75	2.515
Ref.	Hunan Team (1976)	Deliens & Piret (1985a,b)	This study

rare in natural uranyl minerals (*e.g.* ewingite, Olds *et al.*, 2016) and synthetic uranyl compounds. Krivovichev & Burns (2002a,b) report the only synthetic inorganic uranyl compound, $Ag_6[(UO_2)_3O(MoO_4)_5]$, that contains sheets made of trimers of uranyl polyhedra that are linked via corner-sharing with other cation polyhedra (Fig. 6f). Isolated trimers of UO_7 bipyramids are observed in the compound $((UO_2)_3O(OH)_3(H_2O)_6)(NO_3)(H_2O)_4$ (Åberg, 1978), and trimers of UO_7 bipyramids that are linked via corner- and edge-sharing with Mo^{6+} polyhedra are known in the structure of $Cs_4[(UO_2)_3O(MoO_4)_2(MoO_5)]$ (Krivovichev & Burns, 2002b).

5.4. Structure topology

The uranyl phosphate sheets, occurring in the furongite structure, show an anion topology with pentagons, triangles, and squares (Fig. 7c). The uranyl pentagonal bipyramids (pentagons) are connected together by edge-sharing to form infinite parallel chains. Adjacent chains of UrO_5 polyhedra are connected by alternating edge-sharing PO_4 tetrahedra (triangles). Connection between the UrO_5 and PO_4 polyhedra leads to the formation of squares, which are not occupied by any
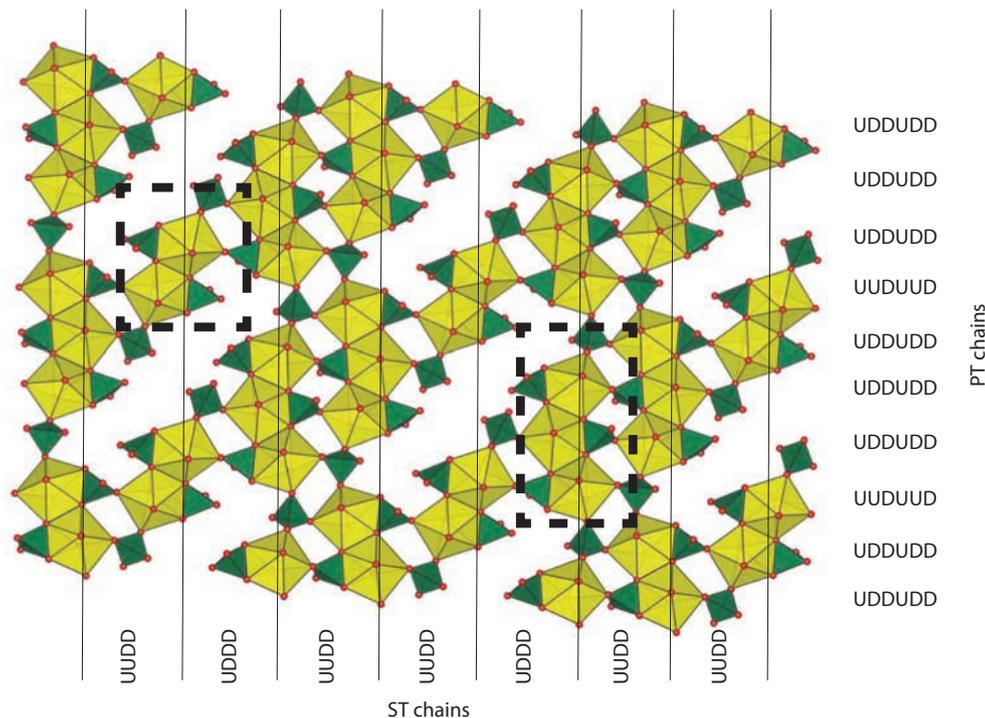
Fig. 5. View of the uranyl phosphate sheet occurring in the structure of furongite. Dimers and trimers of uranyl pentagonal bipyramids are outlined by the dashed lines. U (up) and D (down) symbolize the orientation of the PO_4 tetrahedra along the ST (square–triangle) and PT (pentagon–triangle) chains.
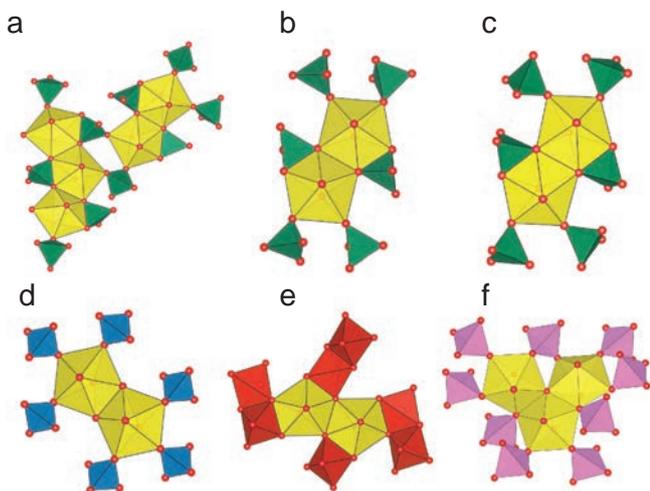
Fig. 6. View of the dimers and trimers of edge-sharing uranyl pentagonal bipyramids in the structure of furongite (a), parsonite (b), lakebogaite (c), plášilite (d), francevillite (e) and $Ag_6[(UO_2)_3O(MoO_4)_5]$ (f). Yellow, UO_7; green, PO_4; blue, SO_4; red, VO_5; and pink, MoO_4 groups.

oxygen atoms with the UrO_5 polyhedra, the two other oxygen atoms are only bonded to Al clusters. In comparison with the uranophane-type sheets, the furongite-type sheets have some UO_7 pentagonal bipyramids missing, leading to the formation of gaps in the sheets. Considering the chains of UrO_5 pentagonal bipyramids and PO_4 tetrahedra, one can see that each three UrO_5 polyhedra, one of them is missing and that all PO_4 tetrahedra are still present (Fig. 7c). Consequently, each gap created corresponds to four missing UrO_5 polyhedra, and contains two $Al_2O_5(OH)(H_2O)_5$ and one $Al_4O_8(OH)_2(H_2O)_{10}$ cluster. Furongite and ulrichite, $Cu[Ca(UO_2)(PO_4)_2(H_2O)_4$, are the only minerals with an uranophane anion topology in which some UO_7 pentagonal bipyramids are replaced by other polyhedra (by CaO_8 in the case of ulrichite). In comparison with uranophane-α, the sheets of furongite are distorted, mainly due to the rotation of the $U2O_7$ pentagonal bipyramids and PO_4 which are connected to the Al clusters. Note that, several neptunium-bearing compounds showing a sheet structure based on deficient versions of uranophane-type sheets were reported (Krivovichev, 2009).

Burns *et al.* (1996) and Kubatko & Burns (2006) explain how minerals with a structure possessing a uranophane anion topology can be distinguished on the basis of the orientations of the tetrahedra along the "horizontal" PT chains (pentagon–triangle) and the "vertical" ST chains (square–triangle) (Fig. 5). In these chains, the apical ligands of the tetrahedra can point either up (U) or down (D). In the furongite sheets, both the ST and PT chains show two kinds of alternating sequences of

cations. Close examination of the polyhedral representation of the sheets indicates that the sheets occurring in the furongite structure are very similar to that of uranophane-α (Ginderow, 1988; Burns *et al.*, 1996). Following the method of Burns *et al.* (1996), the sheet-anion topology of the furongite can easily be constructed from the uranophane anion topology (Fig. 7). However, as some pentagons remain vacant, some PO_4 tetrahedra disappear from the topological construction as they share only two

Fig. 7. The process for transforming the sheet anion topology of uranophane-α (a) into that of furongite (c).

the phosphate tetrahedra. Along the ST chains, the tetrahedra alternate as UUDD and as UDDD, whereas those along the PT chains alternate as UDDUDD and UUDUUD. The sequence UUDD observed in the ST chains is the same as the sequence observed in the ST chains of uranophane-β. The three other sequences (UDDD, UDDUDD, and UUDUUD) are not observed in any other mineral with the uranophane anion topology. In conclusion, all these structural and topological observations indicate that furongite is a new geometrical isomer of the uranophane group.

6. Conclusion

The crystal structure of furongite has been solved for the first time, giving the structural formula $Al_4[(UO_2)_4(PO_4)_6](OH)_2(H_2O)_{19.5}$, or the simplified form $Al_2[(UO_2)_2(PO_4)_3](OH)(H_2O)_{10}$. The chemical composition measured by Deliens & Piret (1985a) is confirmed, except for the water content which is lower in the present study. The crystal structure of furongite is remarkable and unique, showing a novel uranyl phosphate sheet with the composition $[(UO_2)_4(PO_4)_6]^{10-}$. These sheets are made of common dimers and very rare trimers of uranyl pentagonal bipyramids connected by alternating edge-sharing PO_4 tetrahedra. Despite these unparalleled features, the anion topology of the furongite-type sheet can easily be derived from the uranophane anion topology, which is observed in the most common uranyl silicate minerals. The occurrence of $Al_2O_5(OH)(H_2O)_5$ and $Al_4O_8(OH)_2(H_2O)_{10}$ clusters running through the uranyl-phosphate sheets is also a novel structural feature.

References

Åberg, M. (1969): The crystal structure of $(UO_2)_2(OH)_2Cl_2(H_2O)_4$. *Acta Chem. Scand.*, **23**, 791–810.

— (1978): The crystal structure of hexaaqua-tri-my-hydroxo-my 3-oxo-triuranyl(VI) nitrate tetrahydrate, $((UO_2)_3O(OH)_3(H_2O)_6)$ $NO_3(H_2O)_4$. *Acta Chem. Scand.*, **32**, 101–107.

Agilent Technologies (2012): CrysAlis CCD and CrysAlis RED. Oxford Diffraction Ltd, Yarnton, Oxfordshire, UK.

Almond, P.M. & Albrecht-Schmitt, T.E. (2004): Hydrothermal synthesis and crystal chemistry of the new strontium uranyl selenites, $Sr[(UO_2)_3(SeO_3)_2O_2]·4H_2O$ and $Sr[UO_2(SeO_3)_2]$. *Am. Mineral.*, **89**, 976–980.

Almond, P.M., Peper, S.M., Bakker, E., Albrecht-Schmitt, T.E. (2002): Variable dimensionality and new uranium oxide topologies in the alkaline-earth metal uranyl selenites *AE* $[(UO_2)(SeO_3)_2]$ (*AE*=Ca, Ba) and $Sr[(UO_2)(SeO_3)_2]·2H_2O$. *J. Solid State Chem.*, **168**, 358–366.

Brown, I.D. & Altermatt, D. (1985): Bond-valence parameters obtained from a systematic analysis of the inorganic crystal structure database. *Acta Crystallogr.*, **B41**, 244–247, with updated parameters from http://www.ccp14.ac.uk/ccp/web-mirrors/i_d_brown/.

Burns, P.C. (2005): U^{6+} minerals and inorganic compounds: insights into an expanded structural hierarchy of crystal structures. *Can. Mineral.*, **43**, 1839–1894.

Burns, P.C., Ewing, R.C., Hawthorne, F.C. (1997): The crystal chemistry of hexavalent uranium: polyhedron geometries, bond-valence parameters, and polymerization of polyhedra. *Can. Mineral.*, **35**, 1551–1570.

Burns, P.C., Miller, M.L., Ewing, R.C. (1996): U^{6+} minerals and inorganic phases: a comparison and hierarchy of crystal structures. *Can. Mineral.*, **34**, 845–880.

Deliens, M. & Piret, P. (1977): Les phosphates d'uranyle et d'aluminium de Kobokobo. I. Données préliminaires. *Bull. Soc. Belge Géol.*, **86**, 183–190.

—, — (1979a): Les phosphates d'uranyle et d'aluminium de Kobokobo. II. La phuralumite $Al_2(UO_2)_3(PO_4)_2(OH)_6·10H_2O$ et l'upalite $Al(UO_2)_3(PO_4)_2(OH)_3$, nouveaux minéraux. *Bull. Minéral.*, **102**, 333–337.

—, — (1979b): Ranunculite, $AlH(UO_2)(PO_4)(OH)_3·4H_2O$, a new mineral. *Mineral. Mag.*, **43**, 321–323.

—, — (1979c): Les phosphates d'uranyle et d'aluminium de Kobokobo. IV. La threadgoldite, $Al(UO_2)_2(PO_4)_2(OH)\cdot 8H_2O$, nouveau minéral. *Bull. Minéral.*, **102**, 338–341

—, — (1981): Les phosphates d'uranyle et d'aluminium de Kobokobo. V. La mundite, nouveau minéral. *Bull. Minéral.*, **104**, 669–671.

—, — (1982): Les phosphates d'uranyle et d'aluminium de Kobokobo. VI. La triangulite, $Al_3(UO_2\cdot PO_4)_4(OH)_5\cdot 5H_2O$, nouveau minéral. *Bull. Minéral.*, **105**, 611–614.

—, — (1984): La kamitugaïte, $PbAl(UO_2)_5[(P,As)O_4]_2(OH)_9\cdot 9,5 H_2O$, nouveau minéral de Kobokobo, Kivu, Zaïre. *Bull. Minéral.*, **107**, 15–19.

—, — (1985a): Les phosphates d'uranyle et d'aluminium de Kobokobo. VIII. La furongite. *Ann. Soc. Géol. de Belgique*, **108**, 365–368.

—, — (1985b): Les phosphates d'uranyle et d'aluminium de Kobokobo. VII. La moreauïte, $Al_3UO_2(PO_4)_3(OH)_2\cdot 13H_2O$, nouveau minéral. *Bull. Minéral.*, **108**, 9–13.

—, — (1986): La kusuïte devient la wakefieldite-(Ce) plombifère. *Bull. Minéral.*, **109**, 305–305.

Ginderow, D. (1988): Structure de l'uranophane alpha, $Ca(UO_2)_2(SiO_3OH)_2\cdot 5H_2O$. *Acta Crystallogr.,* **C44**, 421–424.

Hunan Team (1976): A new mineral discovered in China. Furongite $Al_2(UO_2)(PO_4)_2(OH)_2.8H_2O$. *Acta Geol. Sin.,* **2**, 203–204.

Hunan Team (1979): The mineralogical investigation of furongite. *Sci. Sin.,* **22**, 199–206.

Hughes, K., Burns, P.C., Kolitsch, U. (2003): The crystal structure and crystal chemistry of uranosphaerite, $Bi(UO_2)O_2OH$. *Can. Mineral.*, **41**, 677–685.

Kampf, A.R., Kasatkin, A.V., Čejka, J., Marty, J. (2015): Plášilite, $Na(UO_2)(SO_4)(OH)\cdot 2H_2O$, a new uranyl sulfate mineral from the Blue Lizard mine, San Juan County, Utah, USA. *J. Geosci.*, **60**, 1–10.

Khosrawan-Sazedj, F. (1982): On the space group of threadgoldite. *Tschermaks Mineral. Petrogr. Mitt.*, **30**, 111–115.

Kraus, W. & Nolze, G. (1996): POWDER CELL − A program for the representation and manipulation of crystal structures and calculation of the resulting X-ray powder patterns. *J. Appl. Crystallogr.*, **29**, 301–303.

Krivovichev, S.V. (2009): Structural crystallography of inorganic oxysalts. Oxford University Press, Oxford, 167–169.

Krivovichev, S.V. & Burns, P.C. (2002a): Synthesis and structure of $Ag_6[(UO_2)_3O(MoO_4)_5]$: a novel sheet of triuranyl clusters and MoO_4 tetrahedra. *Inorg. Chem.*, **41**, 4108–4110.

—, — (2002b): Crystal chemistry of uranyl molybdates. VI. New uranyl molybdates units in the structures of $Cs_4[(UO_2)_3O(MoO_4)_2(MoO_5)]$ and $Cs_6[(UO_2)(MoO_4)_4]$. *Can. Mineral.*, **40**, 201–209.

Kubatko, K.A. & Burns, P.C. (2006): A novel arrangement of silicate tetrahedra in the uranyl silicate sheet of oursinite, $(Co_{0.8}Mg_{0.2})[(UO_2)(SiO_3OH)]_2(H_2O)_6$. *Am. Mineral.,* **91**, 333–336.

Locock, A.J., Burns, P.C., Flynn, T.M. (2005): The role of water in the structures of synthetic hallimondite, $Pb_2[(UO_2)(AsO_4)_2](H_2O)_n$ and synthetic parsonsite, $Pb_2[(UO_2)(PO_4)_2](H_2O)_n$, $0 \le n \le 0.5$. *Am. Mineral.*, **90**, 240–246.

Mereiter, K. (1982): Die Kristallstruktur des Johannits, $Cu(UO_2)_2(OH)_2(SO_4)_2\cdot 8(H_2O)$. *Tschermaks Mineral. Petrogr. Mitt.*, **30**, 47–57.

— (1986): Crystal structure refinement of two francevillites, $(Ba, Pb)[(UO_2)_2V_2O_8]\cdot 5H_2O$. *N. Jb. Mineral. Mh.*, **1986**, 552–560.

Mills, S.J., Birch, W.D., Kolitsch, U., Mumme, W.G., Grey, I.E. (2008): Lakebogaite, $CaNaFe^{3+}_2H(UO_2)_2(PO_4)_4(OH)_2(H_2O)_8$, a new uranyl phosphate with a unique crystal structure from Victoria, Australia. *Am. Mineral.*, **93**, 691–697.

Mills, S.J., Birch, W.D., Kampf, A.R., van Wambeke, L. (2010): Kobokoboite, $Al_6(PO_4)_4(OH)_6\cdot 11H_2O$, a new mineral from the Kobokobo pegmatite, Democratic Republic of the Congo. *Eur. J. Mineral.*, **22**, 305–308.

Momma, K. & Izumi, F. (2011): VESTA 3 for three-dimensional visualization of crystal, volumetric and morphology data. *J. Appl. Crystallogr.*, **44**, 1272–1276.

Olds, T.A., Plášil, J., Kampf, A.R., Burns, P.C., Simonetti, A., Sadergaski, L.R. (2016): Ewingite, IMA 2016-012. CNMNC Newsletter No. 31, June 2016, page 697. *Mineral. Mag.,* **80**, 691–697.

Piret, P. & Declercq, J.-P. (1983): Structure cristalline de l'upalite $Al[(UO_2)_3O(OH)(PO_4)_2]\cdot 7H_2O$. Un exemple de macle mimétique. *Bull. Minéral.*, **106**, 383–389.

Piret, P. & Deliens M. (1982): La vanmeerscheite $U(UO_2)_3(PO_4)_2(OH)_6\cdot 4(H_2O)$ et la méta-vanmeerscheite $U(UO_2)_3(PO_4)_2(OH)_6\cdot 2(H_2O)$, nouveaux minéraux. *Bull. Minéral.*, **105**, 125–128.

—, — (1987): Les phosphates d'uranyle et d'aluminium de Kobokobo IX. L'althupite $AlTh(UO_2)[(UO_2)_3O(OH)PO_4)_2]_2(OH)_3\cdot 15H_2O$, nouveau minéral; propriétés et structure cristalline. *Bull. Minéral.*, **110**, 65–72.

Piret, P., Piret-Meunier, J., Declercq, J.-P. (1979): Structure of phuralumite. *Acta Crystallogr. B*, **35**, 1880–1882.

Plášil, J., Hauser, J., Petříček, V., Meisser, N., Mills, S.J., Škoda, R., Fejfarová, K., Čejka, J., Sejkora, J., Hloušek, J., Johannet, J.-M., Machovič, V., Lapčák, L. (2012): Crystal structure and formula revision of deliensite, $Fe[(UO_2)_2(SO_4)_2(OH)_2](H_2O)_7$. *Mineral. Mag.*, **76**, 2837–2860.

Rosenzweig, A. & Ryan, R.R. (1977): Vandenbrandeite $CuUO_2(OH)_4$. *Cryst. Struct. Commun.*, **6**, 53–56.

Safiannikoff, A. & van Wambeke, L. (1967): La pegmatite radioactive à béryl de Kobokobo et les autres venues pegmatitiques et filoniennes de la région de Kamituga − Kivu − Rép. du Congo. *Mineral. Deposita*, **2**, 119–130.

Serezhkina, L.B., Trunov, V.K., Kholodkovskaya, L.N., Kuchumova, N.V. (1990): Crystal structure of $KUO_2CrO_4(OH)\cdot 1.5(H_2O)$. *Koord. Khim. (= Coordination Chem. (USSR))*, **16**, 1288–1291.

Sheldrick, G.M. (2008): A short history of SHELX. *Acta Crystallogr.*, **A64**, 112–122.

— (2015): Crystal structure refinement with SHELXL. *Acta Crystallogr.*, **C71**, 3–8.

Shen, J. & Peng, Z. (1981): The crystal structure of furongite. *Acta Crystallogr.*, **A37**, 186.

van Wambeke, L. (1972): Eylettersite, un nouveau phosphate de thorium appartenant à la série de la crandallite. *Bull. Soc. fr. Minéral. Cristallogr.*, **95**, 98–105.

Wilson, A.J.C. (1992): International Tables for X-ray Crystallography, vol. C. Kluwer Academic Press, London, 883 p.